Self-trapped spatiotemporal necklace-ring solitons in the Ginzburg-Landau equation

Y. J. He, H. H. Fan, J. W. Dong, and H. Z. Wang*
State Key Laboratory of Optoelectronic Materials and Technologies, Zhongshan (Sun Yat-Sen) University, Guangzhou 510275, China
(Received 18 October 2005; revised manuscript received 5 May 2006; published 28 July 2006)

We consider a class of self-trapped spatiotemporal solitons: spatiotemporal necklace-ring solitons, whose intensities are azimuthally periodically modulated. We reveal numerically that the spatiotemporal necklace-ring solitons carrying zero, integer, and even fractional angular momentum can be self-trapped over a huge propagation distance in the three-dimensional cubic-quintic complex Ginzburg-Landau equation, even in the presence of random perturbations.

DOI: 10.1103/PhysRevE.74.016611 PACS number(s): 42.65.Tg, 05.45.Yv

I. INTRODUCTION

A necklace-ring beam is a ring-shaped beam with a periodic intensity change along the azimuthal direction and the intensity spots within the ring look like pearls in a necklace. It was first observed in experiment that necklace-ring beams exist as stable entities propagating in Kerr medium [1]. It has also been found theoretically that such a necklace-ring beam can exhibit quasistable propagation in a self-focusing Kerr medium [2–4]. However, it is well known that (2+1)-dimensional [(2+1)D] (two transverse plus one longitudinal dimensions) solitons in self-focusing Kerr medium are inherently unstable [5]. Necklace-ring vector solitons exhibit also quasistable propagation in a saturable nonlinearity medium [6]. Stable (2+1)D necklace-ring solitons (NRSs) carrying zero, integer, and even fractional angular momentum have also been investigated [4,6]. In more recent experiment, NRSs exist as stationary propagation in a two-dimensional (2D) optically induced lattice [7]. NRSs can be also thought of as a superposition of two rings carrying equal but opposite topological charge [4]. Such a necklace-ring pattern allows the beam to transport several times the critical power for self-focusing before critical breakdown.

We stress that the NRSs are different from the soliton clusters composed of several interacting solitons [8], because in soliton clusters adjacent solitons are uniform in phase and, therefore, the neighboring solitons attract mutually. This is in contrast to the case of NRSs. In NRSs, each pearl is not a soliton and adjacent bright pearls on the ring structure differ in phase by π and, therefore, the neighboring pearls repulse each other [3]. In NRSs, it is the interaction between the pearls that stabilizes the structure as a whole. As shown in Ref. [3], an isolated individual pearl is highly unstable. However, it is difficult for the NRSs to exist as stationary self-trapped structures in propagation for a large distance, and they expand with propagation because adjacent pearls differ in phase by π [3].

In addition, all these theoretical and experimental studies were performed merely about 2D NRSs; however, the investigation of spatiotemporal [i.e., (3+1)D] (two spatial, one temporal and plus one longitudinal dimensions) NRSs has not been found yet. It is well known that spatiotemporal optical solitons, the so-called light bullets localized in all spatial and time dimensions are more challenging objects for fundamental research due to the possibility of violet collapse in a self-focusing medium in higher dimensions [9,10]; therefore, the formation of stable localized objects in (3+1)D nonlinear fields is difficult in physics. Spatiotemporal optical solitons have attracted a lot of attention in the last several years [11].

The complex Ginzburg-Landau (GL) equation is known to play a universal role in science. This equation is encountered in several diverse branches of physics, such as in superconductivity and superfluidity, nonequilibrium fluid dynamics and chemical systems, nonlinear optics, Bose-Einstein condensates, and in quantum field theories [12–16]. The theory of pulses in various (1+1)D and (2+1)D models of the GL type was well elaborated [17–19]; much less is known about (3+1)D localized patterns or bright solitons.

In this paper, by performing simulations using the (3+1)D cubic-quintic (CQ) complex GL equation, we obtain self-trapped spatiotemporal NRSs carrying zero, integer, and even fractional angular momentum. It is indeed easy to find the spatiotemporal NRSs can be self-trapped over a large propagation distance against all the perturbations, including an azimuthal one which is fatal for the nonlinear Schrödinger (NLS) equation vortex ring.

II. THE MODEL AND SOLITONS SOLUTION

We consider the (3+1)D CQ complex GL equation in a general form

$$iu_Z + i\alpha u + (1/2 - i\beta)(u_{XX} + u_{YY} + u_{TT}) + (1 - i\varepsilon)|u|^2 u - (\nu - i\mu)|u|^4 u = 0, \quad (1)$$

where α and μ are the linear and quintic loss parameters (the latter one accounts for the nonlinear gain saturation in optical media), respectively. ε is the cubic gain parameter (which arises, e.g., from saturable absorption), ν is the quintic self-defocusing coefficient, the diffraction and cubic self-focusing coefficients are normalized to be 1. β is diffusion coefficient. It is not a standard part of the propagation equation for optical media, but it appears if light creates free charge carriers [20], which can take place, e.g., in semiconductor waveguides [21]. Due to their physical meaning, all

*Author to whom correspondence should be addressed. Email address: stswhz@zsu.edu.cn

these coefficients are positive. When $\alpha=\beta=\varepsilon=\mu=0$, Eq. (1) becomes a CQ NLS equation which is a conservative version.

The quintic terms added to the system are necessary to stabilize the solitons and background instability [17,18]. The quintic self-defocusing coefficient ν prevents the solitons collapse. The combination of a quintic loss parameter μ and a cubic gain parameter ε provides for the overall stabilization of the model. The quintic terms ensure that the CQ complex GL equation possesses stable spatiotemporal soliton solutions, but which is only one of the required crucial conditions for stabilizing spatiotemporal NRSs carrying angular momentum. In addition, soliton interactions can be controlled by the diffusion coefficient β, which has been demonstrated in the (2+1)D CQ complex GL equation [17]. Thus we predict that the repelling of adjacent pearls in the necklace-ring solitons may be also overcome by the diffusion coefficient. Therefore, we perform numerically simulations using the CQ complex GL equation rather than the CQ NLS equation where the diffusion coefficient is absent.

According to the solution form in Refs. [2,4], we choose the spatiotemporal NRSs shape in

$$u(Z=0,r,\theta)=A\ \mathrm{sech}[\sqrt{(r-R_0)^2+T^2}/w]\cos(\Omega\theta)\exp(im\theta), \tag{2}$$

where A, R_0, w, are initial amplitude, radius and radial width, respectively. Ω determines the period of azimuthal modulation. m is topological charge. r and θ are polar coordinates in the plane (X,Y). The energy is

$$E=\int_{-\infty}^{+\infty}\int_{-\infty}^{+\infty}\int_{-\infty}^{+\infty}|u|^2dXdYdT. \tag{3}$$

The Z component of the angular momentum is

$$L_Z=\int_{-\infty}^{+\infty}\int_{-\infty}^{+\infty}\int_{-\infty}^{+\infty}(\partial\phi/\partial\theta)|u|^2dXdYdT, \tag{4}$$

where ϕ is the phase of u. The evolution of the soliton mean radius $R(Z)$ and soliton mean angular velocity $\omega(Z)$ are monitored. These quantities were defined as follows:

$$R(Z)=E^{-1}\int_{-\infty}^{+\infty}\int_{-\infty}^{+\infty}\int_{-\infty}^{+\infty}(X^2+Y^2)^{1/2}|u|^2dXdYdT, \tag{5}$$

and

$$\omega(Z)=L_Z/I, I=\int_{-\infty}^{+\infty}\int_{-\infty}^{+\infty}\int_{-\infty}^{+\infty}(X^2+Y^2)|u|^2dXdYdT. \tag{6}$$

III. DIRECT SIMULATIONS

Our direct simulations of Eq. (1) are based on slit-step Fourier method with the longitudinal step size $\Delta Z=0.1$ in all cases below. To further study the NRSs' robustness, we add a noise to the input NRSs through multiplying them by width $[1+\rho_{1,2}(X,Y,T)]$, where $\rho_{1,2}(X,Y,T)$ is a Gaussian random function with $\langle\rho_{1,2}\rangle=0$ and $\langle\rho_{1,2}^2\rangle=\sigma_{1,2}^2$ (here we take $\sigma_{1,2}=0.15$). Figures 1(a) and 1(b) show the evolutions of spatiotemporal NRSs carrying, respectively, zero ($m=0$) and integer ($m=6$) angular momentum for a large distance up to $Z=1000L_D$ (L_D is dispersion or diffraction length) in the presence of noise. Input solitons' shapes are $u(Z=0,r,\theta)=1.2\ \mathrm{sech}[\sqrt{(r-R_0)^2+T^2}/2]\cos(6\theta)$. The typical parameters are $\alpha=0.5$, $\beta=0.5$, $\varepsilon=2.52$, $\nu=0.1$, $\mu=1$ and the initial radius $R_0=20$. To overcome the solitons expanding, we choose large value $\beta=0.5$ as a primary control parameter. Figures 1(c) and 1(d) show the evolutions of the mean radii of Figs. 1(a) and 1(b), respectively, as a function of the propagation distance. We realize that in the initial stage for $m=0$, the mean radius rapidly increases to $R=20.20$ due to the repulsion between adjacent pearls, and then greatly decreases due to the control of the diffusion coefficient. After $Z\approx 80L_D$ the expanding and shrinking of the NRS obtain a balance, and the mean radius maintains at $R\approx 20.07$. While for integer angular momentum $m=6$, the mean radius rapidly increases to $R=20.18$ in the initial stage due to both the repulsion between adjacent pearls and the centrifugal force (the angular momentum produces centrifugal force). After $Z=60L_D$ the expanding is suppressed by the diffusion coefficient, and the mean radius maintains at $R\approx 19.82$. Figures 1(e) and 1(f) show the evolutions of angular velocity with the propagation distance for $m=0$ and $m=6$, respectively. For $m=6$, the angular velocity is not a constant, which slightly oscillates and exhibits a very low value along the propagation distance. This property is the result of the dissipative nature of the model. The angular velocity monitored is very small up to $\omega=0.000\ 23$ approximately and the total rotation angle of the NRS is $\theta=0.26$ rad at $Z=1000L_D$. However, the low angular velocity will not decay to zero forever. So it does not imply that the final state is a solution of $m=0$. In both cases, the changes of mean radii are less than 1% of the initial radii and the total energies do not significantly change, i.e., such spatiotemporal NRSs are self-trapped for a large propagation distance (at least $Z=1000L_D$), even in the presence of azimuthal perturbation ($m=6$). When the separations of adjacent pearls are too small, which can be achieved through decreasing the radius or increasing the number of pearls, most energies are concentrated on a few pearls. For example, the allowable minimum separations between pearls for self-trapped spatiotemporal NRSs correspond to the minimum radius $R_0^{min}=16.5$ for $m=0$ and $R_0^{min}=16.8$ for $m=6$. In this case, most energies are concentrated on four pearls periodically distributed on the necklace while other pearls become small [Figs. 2(a) and 2(b)]. If the separations between pearls further become smaller than the cases above, the four pearls become larger and other pearls vanish. The evolutions of their mean radii indicate only a very slight oscillation [Figs. 2(c) and 2(d)].

Figure 3(a) shows the evolution of spatiotemporal NRS carrying fractional angular momentum versus propagation distance in the presence of noise. We launch

$$u(Z=0,r,\theta)=1.2\ \mathrm{sech}[\sqrt{(r-R_0)^2+T^2}/2]\exp(4i\theta)+1.2\ \mathrm{sech}[\sqrt{(r-R_0)^2+T^2}/2]\exp(-i\theta),$$

here $R_0=12$. Such an NRS has a fractional angular momen-

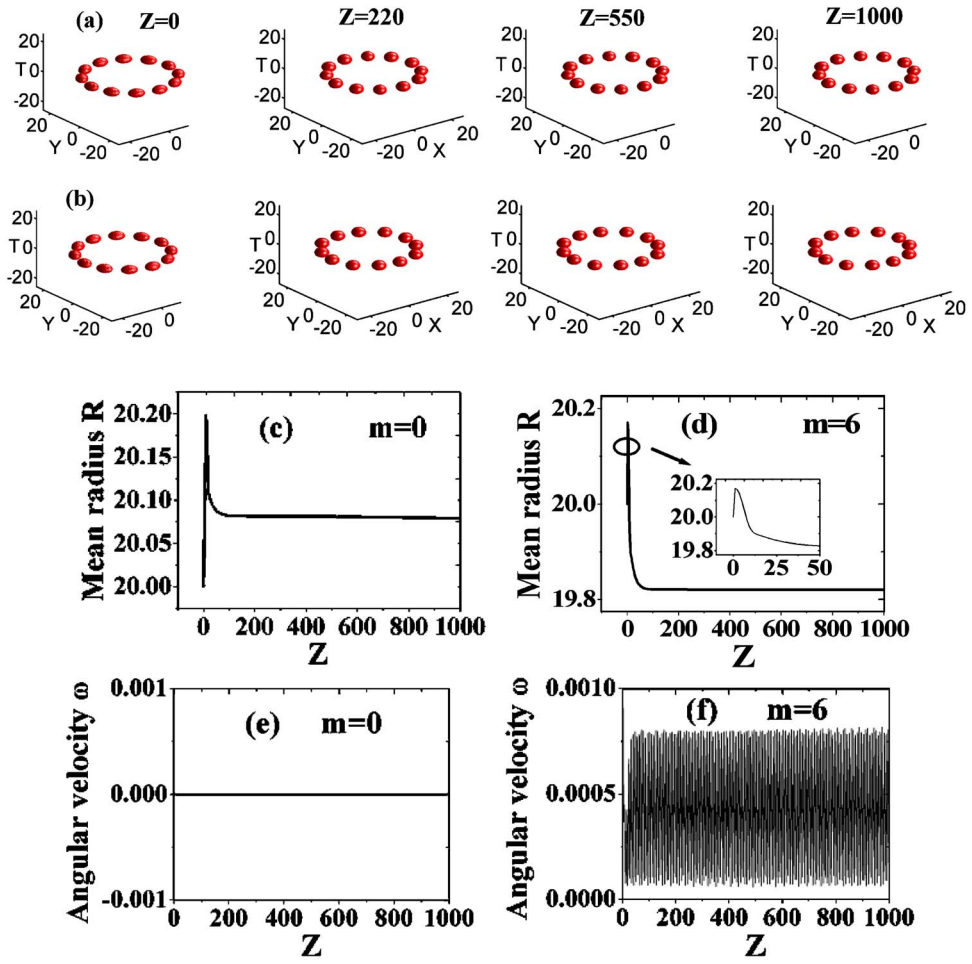

FIG. 1. (Color online) The evolutions of the spatiotemporal necklace-ring solitons (NRSs) carrying, respectively, (a) $m=0$ and (b) $m=6$ angular momentum vs the distance in the presence of noise. (a) and (b) The isosurfaces $|u|=0.6$. The parameters are $A=1.2$, $w=2$, $\Omega=6$, and $R_0=20$. (c) and (d) The evolutions of the mean radii corresponding to $m=0$ and $m=6$, respectively, as a function of the propagation distance. (e) and (f) show the evolutions of the angular velocity with the propagation distance for $m=0$ and $m=6$, respectively.

tum with $L_Z/E_0=m=1/2$. Figure 3(b) shows that the mean radius rapidly increases to $R=12.58$ in the initial stage due to both the repulsion between adjacent pearls and the centrifugal force. After $Z=200L_D$, the expanding is suppressed mainly by the diffusion coefficient, and the mean radius maintains at $R\approx 12.39$. The angular velocity monitored is large before $Z=10L_D$ and after $Z=200L_D$ the angular velocity become very small up to $\omega=0.000\,13$ approximately; the

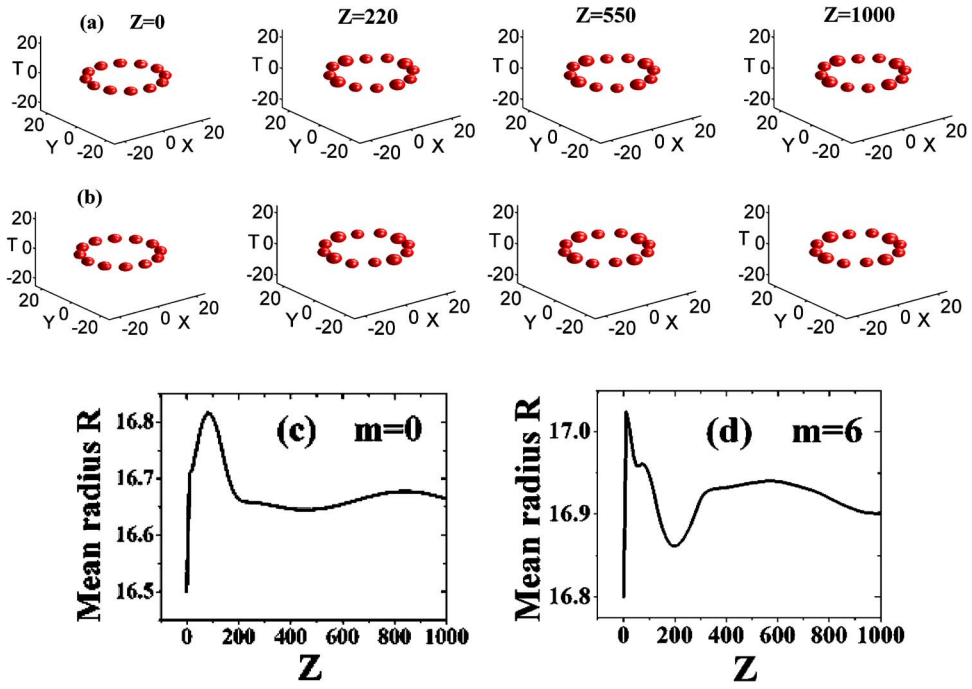

FIG. 2. (Color online) The evolutions of the spatiotemporal NRSs with minimum initial radius. (a) and (c) $m=0$, (b) and (d) $m=6$. The other parameters are the same as in Fig. 1.

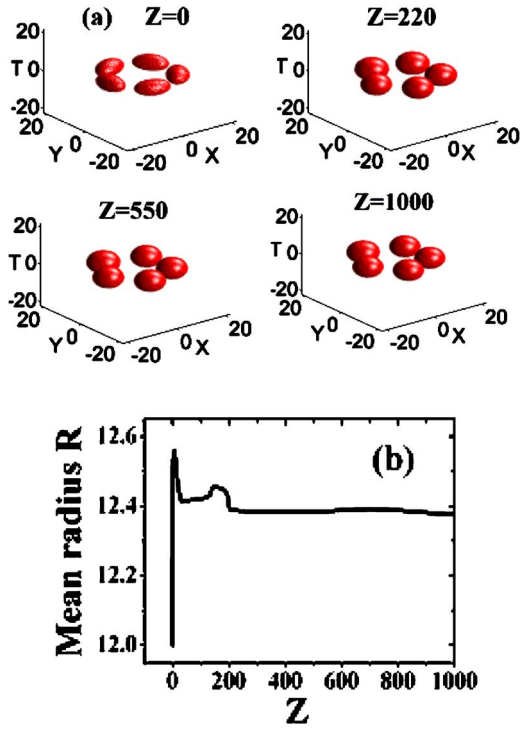

FIG. 3. (Color online) The evolution of the spatiotemporal NRS carrying fractional ($m=L_Z/E_0=1/2$) angular momentum vs the propagation distance in the presence of noise. (a) The isosurfaces $|u|=0.6$. The parameters are $A=1.2$, $w=2$, $R_0=12$, and $\varepsilon=2.56$. The other parameters are the same as in Fig. 1. (b) The evolution of the mean radius as a function of the propagation distance.

total rotation angle of the NRS is $\theta=0.16$ at $Z=1000L_D$. Thus the spatiotemporal NRS carrying fractional angular momentum is self-trapped against perturbations over a large propagation distance.

The physical mechanisms of stabilizing these spatiotemporal NRSs are (i) the simultaneous balances of diffraction and group-velocity dispersion by the transverse self-focusing and self-defocusing and the longitudinal nonlinear phase modulation, respectively; (ii) the gain balances out the linear and quintic losses; (iii) the diffusion coefficient β effectively controls the expanding of necklaces.

In spite of the pearls' initial shape and angular momentum, an interesting property of spatiotemporal NRSs is that after a few L_D's, the initial shape of each pearl evolves into a circular shape, and the circular shape is an attractor. One of the requirements for the stability of these NRSs in the CQ complex GL equation is that azimuthal width of the pearls has to be larger than the radial width of the pearls. This is in contrast to the case of the (2+1)D NRSs in the NLS equation [1–4,6]. This is the consequence of the dissipative nature of the GL equation, as it is explained above. Another requirement for the stabilization of these NRSs is that the radius of any necklace should be larger than its thickness, which is the same as in (2+1)D NRSs[1–4,6].

We show the existent stable/unstable domains in the parameter plane (ε,μ) for the stability of these NRSs [Fig. 4(a)]. In the black region of Fig. 4(a), there coexist stable NRSs carrying zero, integer ($m=6$), and fractional

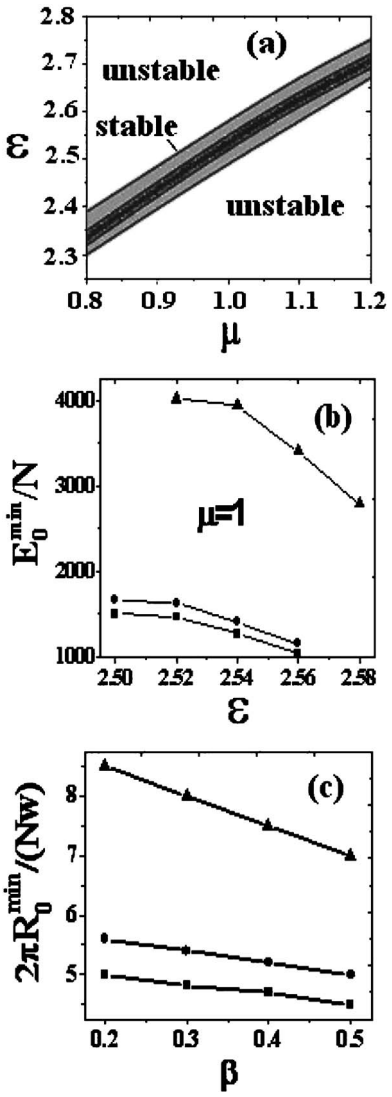

FIG. 4. (a) The existent stable/unstable domains in the parameter plane (ε,μ) for these NRSs carrying zero and nonzero angular momentum. (b) The minimum energy E_0^{min}/N of each pearl vs the cubic gain for a fixed quintic loss. (c) The ratio $2\pi R_0^{min}/(Nw)$ of minimum separation of the adjacent pearls to the pulse width w versus the effective diffusion coefficient β. In (b) and (c) the squares, circles, and triangles correspond to zero, integer ($m=6$), and fractional ($m=1/2$) angular momentum, respectively.

($m=1/2$) angular momentum. In the lower gray region there exist both stable NRSs carrying zero and integer ($m=6$). Whereas in the upper gray region only the stable NRS carrying fractional ($m=1/2$) angular momentum is found to form. Figure 4(b) shows the initial minimum energy E_0^{min}/N of each pearl versus the cubic gain ε for a fixed quintic loss $\mu=1$, where E_0^{min} is minimum total energy corresponding to the initial radius R_0^{min} of the stable NRSs and N is the pearl number in the necklace. The other parameters are $\alpha=0.5$, $\beta=0.5$, and $\nu=0.1$. We plot the ratio $2\pi R_0^{min}/(Nw)$ of minimum separation $2\pi R_0^{min}/N$ of adjacent pearls to the width w versus the effective diffusion coefficient β in Fig. 4(c). The other parameters are $\alpha=0.5$, $\mu=0.1$, $\varepsilon=2.55$, and $\nu=0.1$. One of the requirements for the stability of these NRSs is

both adjacent pearls separation must be larger than the initial minimum $2\pi R_0^{min}/N$ for fixed w and the initial energy of each pearl must be larger than the initial minimum E_0^{min}/N. From Fig. 4(c), when the effective diffusion coefficient β is larger, the $2\pi R_0^{min}/(Nw)$ becomes smaller. This indicates that the expanding of NRSs are easier to be controlled by using a larger value of diffusion coefficient. We must stress that all these NRSs will be unstable for $\beta > 0.55$. For single solitons, there exist different stable regions in Figs. 4(a) and 4(b) in terms of the same parameters.

The CQ complex GL equation can arise in the semiconductor material, where the quintic terms can account for the gain and nonlinearity saturation of the lasing medium; the cubic gain can arise from saturable absorption; the original saturable nonlinearity of the system should be written in terms of a CQ expansion. In addition, in a 2D array of vertical-cavity surface emitting lasers, at which the nonlinear medium involved a (resonant) laser medium, so the underlying equation is also the complex GL equation. By use of a bulk laser medium (3D), these systems can be related to the model described by Eq. (1). There is only preliminary experimental work on demonstration of light bullets in quadratic nonlinear media [22], where the light bullets are 2D spatiotemporal solitons instead of 3D spatiotemporal solitons.

IV. CONCLUSION

In conclusion, we have presented a different class of spatiotemporal solitons: spatiotemporal necklace-ring solitons. By selecting proper parameters in the (3+1D) CQ complex GL equation, we have proven that the spatiotemporal necklace-ring solitons carrying zero or nonzero angular momentum can be self-trapped for a very large distance. This class of self-trapped spatiotemporal solitons are of fundamental interest because the CQ complex GL equation appears in many physical settings. For example, it can also describe the dynamics of open Bose-Einstein condensates (BECs). The dissipation of the BECs, as shown in Eq. (1), can naturally occur in an open condensate; while the gains can arise from the interaction between the condensed and the uncondensed atoms [23,24]. So our results may be useful to study the similar solitons in BECs, e.g., the necklace pattern of vortex pairs predicted theoretically in a BECs model [25]. Recently, two-dimensional two-component bright solitons of an annular shape with hidden and explicit vorticities in the components could be stabilized in media with the cubic-quintic nonlinearity [26], and new generic types of vorticity-carrying soliton complexes in a class of physical systems, including an attractive Bose-Einstein condensate in a square optical lattice and photonic lattices in photorefractive media, were also demonstrated to be stable [27]. The patterns include ring-shaped higher-order vortex solitons and supervortices.

ACKNOWLEDGMENTS

This work is supported by the National 973 (Grant No. 2004CB719804) Project of China, the National Natural Science Foundation of China (Grant No. 10274108), and the Natural Science Foundation of Guangdong Province of China.

[1] A. Barthelemy, C. Froehly, and M. Shalaby, Proc. SPIE **2041**, 104 (1993).
[2] M. Soljačić and M. Segev, Phys. Rev. Lett. **81**, 4851 (1998).
[3] M. Soljačić and M. Segev, Phys. Rev. E **62**, 2810 (2000).
[4] M. Soljačić and M. Segev, Phys. Rev. Lett. **86**, 420 (2001).
[5] P. L. Kelley, Phys. Rev. Lett. **15**, 1005 (1965).
[6] A. S. Desyatnikov and Yu. S. Kivshar, Phys. Rev. Lett. **87**, 033901 (2001).
[7] J. Yang, I. Makasyuk, P. G. Kevrekidis, H. Martin, B. A. Malomed, D. J. Frantzeskakis, and Zhigang Chen, Phys. Rev. Lett. **94**, 113902 (2005).
[8] A. S. Desyatnikov and Yu. S. Kivshar, Phys. Rev. Lett. **88**, 053901 (2002).
[9] B. Gross and J. T. Manassah, Opt. Commun. **129**, 143 (1996).
[10] L. Berge, Phys. Rep. **303**, 260 (1998).
[11] Boris A. Malomed, Dumitru Mihalache, Frank Wise, and Lluis Torner, J. Opt. B: Quantum Semiclassical Opt. **7**, R53 (2005).
[12] Y. Kuramoto, *Chemical Oscillations, Waves and Turbulence* (Springer, Berlin, 1984).
[13] P. Manneville, *Dissipative Structures and Weak Turbulence* (Academic, San Diego, 1990).
[14] M. C. Cross and P. C. Hohenberg, Rev. Mod. Phys. **65**, 851 (1993).
[15] N. N. Akhmediev and A. Ankiewicz, *Solitons, Nonlinear Pulses and Beams* (Chapman and Hall, London, 1997).
[16] A. M. Sergeev and V. I. Petviashvili, Dokl. Akad. Nauk SSSR **276**, 1380 (1984) [Sov. Phys. Dokl. **29**, 493 (1984)].
[17] Dmitry V. Skryabin and Andrei G. Vladimirov, Phys. Rev. Lett. **89**, 044101 (2002).
[18] Boris A. Malomed, Phys. Rev. E **58**, 7928 (1998).
[19] L.-C. Crasovan, B. A. Malomed, and D. Mihalache, Phys. Rev. E **63**, 016605 (2000).
[20] L.-C. Crasovan, B. A. Malomed, and D. Mihalache, Phys. Lett. A **289**, 59 (2001).
[21] K. Otsuka, *Nonlinear Dynamics in Optical Complex Systems* (KTK Scientific Publishers, Tokyo, 1999).
[22] X. Liu, L. J. Qian, and F. W. Wise, Phys. Rev. Lett. **82**, 4631 (1999).
[23] B. Kneer, T. Wong, K. Vogel, W. P. Schleich, and D. F. Walls, Phys. Rev. A **58**, 4841 (1998).
[24] F. T. Arecchi, J. Bragard, and L. M. Castellano, in *Bose-Einstein Condensates and Atom Lasers* (Kluwer, New York, 2002).
[25] G. Theocharis, D. J. Frantzeskakis, P. G. Kevrekidis, B. A. Malomed, and Yuri S. Kivshar, Phys. Rev. Lett. **90**, 120403 (2003).
[26] A. S. Desyatnikov, D. Mihalache, D. Mazilu, B. A. Malomed, C. Denz, and F. Lederer, Phys. Rev. E **71**, 026615 (2005).
[27] H. Sakaguchi and B. A. Malomed, Europhys. Lett. **72**, 698 (2005).